Journal of Power Sources 629 (2025) 235901

Contents lists available at ScienceDirect

Journal of Power Sources

journal homepage: www.elsevier.com/locate/jpowsour

Real-vehicle experimental validation of a predictive energy management strategy for fuel cell vehicles

Sandro Kofler [a,*], Georg Rammer [b], Alexander Schnabel [b], David Weingrill [b], Peter Bardosch [b], Stefan Jakubek [a], Christoph Hametner [a]

[a] Institute of Mechanics and Mechatronics, TU Wien, Getreidemarkt 9, Vienna, 1060, Austria
[b] AVL List GmbH, Hans-List-Platz 1, Graz, 8020, Austria

HIGHLIGHTS

- Long-term predictions are used to optimize a battery SoC reference trajectory.
- Application-oriented experimental validation with a real fuel cell vehicle.
- Real driving tests on public roads affected by real-world influences such as traffic.
- Direct comparison with a nonpredictive method in reproducible dynamometer tests.
- Significant reduction in fuel consumption by 6.4 %.

ARTICLE INFO

Keywords:
Experimental validation
Fuel cell vehicle
Optimized SoC reference
Predictive energy management
Real driving test

ABSTRACT

Predictive information is highly valuable for energy management strategies (EMSs) of fuel cell vehicles. In particular, long-term predictions can significantly improve the fuel efficiency because they allow for an optimization of the energy management before departure. This potential has been demonstrated in numerous simulation studies. This work extends the literature with an extensive experimental validation of a predictive EMS that exploits route-based long-term predictions in the form of optimized reference trajectories for the battery state of charge. The experimental validation is performed with a real passenger fuel cell vehicle and strongly focuses on the real-world application where random influences such as traffic cause considerable disturbances with respect to the long-term prediction. The validation comprises two stages: First, real driving tests are repeatedly conducted on public roads, analyzing the robustness of the predictive EMS and assessing fuel efficiency gains over a nonpredictive EMS. Second, chassis dynamometer tests are performed where a selected real driving cycle is reproduced to compare the two EMSs directly. The chassis dynamometer tests confirm a significant reduction in the fuel consumption by 6.4 % compared to the nonpredictive EMS. The experimental results are analyzed quantitatively and qualitatively in detail.

1. Introduction

Fuel cell vehicles commonly have a hybrid powertrain consisting of the fuel cell system (FCS) and a battery (see Fig. 1), and the power allocation between the two power sources is determined with an energy management strategy (EMS). The EMS has a direct impact on the operating ranges of the two powertrain components and can strongly influence the fuel efficiency by avoiding inefficient operation. In addition to fuel efficiency, ensuring feasible operation is important: The requested system power must be satisfied within reasonable time, and powertrain constraints, such as constraints on the battery state of charge (SoC), must not be violated.

The optimal energy management in view of these aspects is highly specific to the power demand profile of the driving mission. Consequently, the performance of an EMS can be enhanced by considering appropriate predictive information of the driving mission. To improve the fuel efficiency by actively involving the battery in the energy management, long prediction horizons are necessary. For example, the optimal energy management for a trip including an ascent could require charging the battery already several kilometers before reaching the

* Corresponding author.
E-mail addresses: sandro.kofler@tuwien.ac.at (S. Kofler), georg.rammer@avl.com (G. Rammer), alexander.schnabel@avl.com (A. Schnabel), david.weingrill@avl.com (D. Weingrill), peter.bardosch@avl.com (P. Bardosch), stefan.jakubek@tuwien.ac.at (S. Jakubek), christoph.hametner@tuwien.ac.at (C. Hametner).

https://doi.org/10.1016/j.jpowsour.2024.235901
Received 10 September 2024; Received in revised form 10 November 2024; Accepted 18 November 2024
Available online 1 December 2024

uphill section. Long-term predictive information can be retrieved from different sources. At a basic level, long-term information can just consist of the trip length, which is often considered in predictive EMSs for plug-in hybrids to achieve an even use of battery energy throughout the driving mission [1–3]. However, the knowledge of the trip length alone does not provide information regarding the power demand profile, which is needed to optimally adapt the energy management to the driving mission. More advanced and yet simply applicable approaches consider static route information, such as the altitude profile, legal speed limits, or average segment speeds, to get long-term estimates of the power demand [4]. Even though such long-term predictions have limited accuracy, they can be highly effective for the energy management because they are available for the entire driving mission in advance. Consequently, the energy management for a planned trip can be optimized before departure, yielding predictive control information that can then be considered in the real-time EMS while driving. In the literature, optimized reference trajectories for the battery SoC have shown to be an effective way to inform the real-time EMS with the long-term prediction. Simple and yet robust strategies directly track the optimized SoC reference with basic control laws to determine the real-time power allocation between the FCS and the battery while considering powertrain constraints [5,6]. An optimization-based alternative is the adaptive equivalent consumption minimization strategy (ECMS). Here, a proportional-integral (PI) controller that tracks the SoC reference trajectory is used to determine the so-called equivalence factor, which expresses a virtual fuel consumption for using energy from the battery [7–9]. The indirect consideration of the SoC feedback combined with the continuous optimization of the equivalent fuel consumption allows for a more gradual adaption of the power allocation, which can benefit the fuel efficiency. Also, ECMS-based methods that additionally consider real-time short-term predictions while tracking the SoC reference trajectory have been developed [10–14]. Similarly, model predictive control (MPC) approaches combine short-term predictions with the long-term prediction in the form of the SoC reference while also taking into account powertrain constraints [2,15–19]. Besides SoC reference trajectories, optimized maps expressing the optimal equivalence factor or the optimal cost-to-go depending on the covered distance and SoC can be used to inform the real-time EMS with the long-term prediction. Such map-based approaches are advantageous when the long-term prediction considerably deviates because they allow the real-time EMS to continuously adapt to the actual conditions and preserve close-to-optimal fuel efficiency. EMSs based on the ECMS [20–22] and MPC [23] have been proposed to consider predictive control information in the form of optimized maps. Regardless of the approach, considering long-term power demand predictions has shown significant fuel efficiency gains over nonpredictive alternatives in simulation-based studies. However, experimental validations with real vehicles on real-world driving missions that confirm these performance benefits are not available in the literature so far.

In general, the early development and performance evaluation of EMSs, predictive and nonpredictive, happens in simulation. Simulation studies are cost and time efficient, but their outcomes deviate from reality because of modeling errors, unconsidered system behavior, and other influences. Validation with hardware-in-the-loop (HIL) testing is more realistic but found less frequently in the literature. The significance of HIL tests grows with their complexity. Simple HIL experiments only consider controller hardware to validate the real-time capability of the EMS and emulate the powertrain behavior, such as in [24–26], whereas more complex HIL setups also include small-scale powertrain components, as for example in [27–30]. Particularly HIL testing with full-scale powertrain components such as in [31–34] comes close to reality but still does not entirely cover the vehicle behavior in real-world driving.

Real driving tests with fully functional vehicles are the ultimate level of validation, but they are rare in the literature due to high cost and effort. For example, small experimental vehicles are used in real driving tests to validate nonpredictive EMSs in [35–37] and a model predictive controller considering short-term predictions in [38]. In [39–41], nonpredictive fuzzy logic strategies are demonstrated and investigated with real fuel cell trucks and buses on public roads. Similarly, extensive road tests with fuel cell buses are conducted in [42–44] to validate further nonpredictive EMSs. Whereas the real vehicle-validated strategies mentioned so far do not take into account long-term predictions, the EMS for plug-in hybrid fuel cell vehicles that was experimentally validated in [45] considers a prediction of the expected energy demand to determine the time when the FCS is turned on. To sum up, real-vehicle validations of EMSs for fuel cell vehicles in the literature were mainly conducted with buses, trucks, and small experimental vehicles and for nonpredictive strategies. In particular, EMSs exploiting long-term power demand predictions to optimize an SoC reference trajectory before departure have not been validated in real-world driving tests with real vehicles so far.

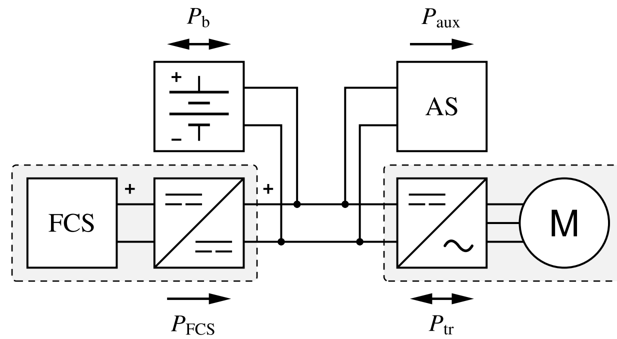

Fig. 1. Hybrid powertrain of the investigated fuel cell vehicle consisting of the FCS, battery, traction motor (M), and auxiliary systems (AS). The arrows indicate the possible directions of the power flows.
Source: The scheme is taken from [23].

The main contribution of this work is an extensive experimental validation of an EMS for fuel cell vehicles that considers a long-term prediction of the power demand to optimize SoC reference trajectories. The experimental validation is conducted with a real fuel cell vehicle and strongly focuses on real-world driving. It comprises two stages, where the performance of the predictive EMS is compared with a nonpredictive charge sustaining strategy (see Fig. 2(a)):

1. Various *real driving tests* are conducted on two routes on public roads. The real driving tests involve all random influences relevant in the actual application, such as dense traffic, traffic regulation, vehicle standstills, and varying driver behavior, which are hardly predictable over a long-term prediction horizon. In addition, the behavior of the real vehicle deviates from the prediction due to model errors. Therefore, the real driving tests evaluate the robustness of the predictive EMS against these unpredicted real-world disturbances and its feasibility regarding specified powertrain constraints. Because the power demand profile varies between individual tests due to the random influences, the performance advantage of the predictive EMS cannot be quantized directly. However, comparisons based on the equivalent fuel consumption, which takes into account differences in the battery energy and energy demand between tests, enable an indirect assessment of the fuel efficiency gains.
2. *Chassis dynamometer tests* based on measurements of a selected *real driving cycle* are conducted. Here, power demand profiles can be reproduced for multiple tests, which allows for a direct performance comparison between the predictive EMS and the nonpredictive EMS. Since the dynamometer tests are based on a real driving cycle and include the entire vehicle, the tests still cover the unpredicted real-world influences and appropriately replicate the actual application.

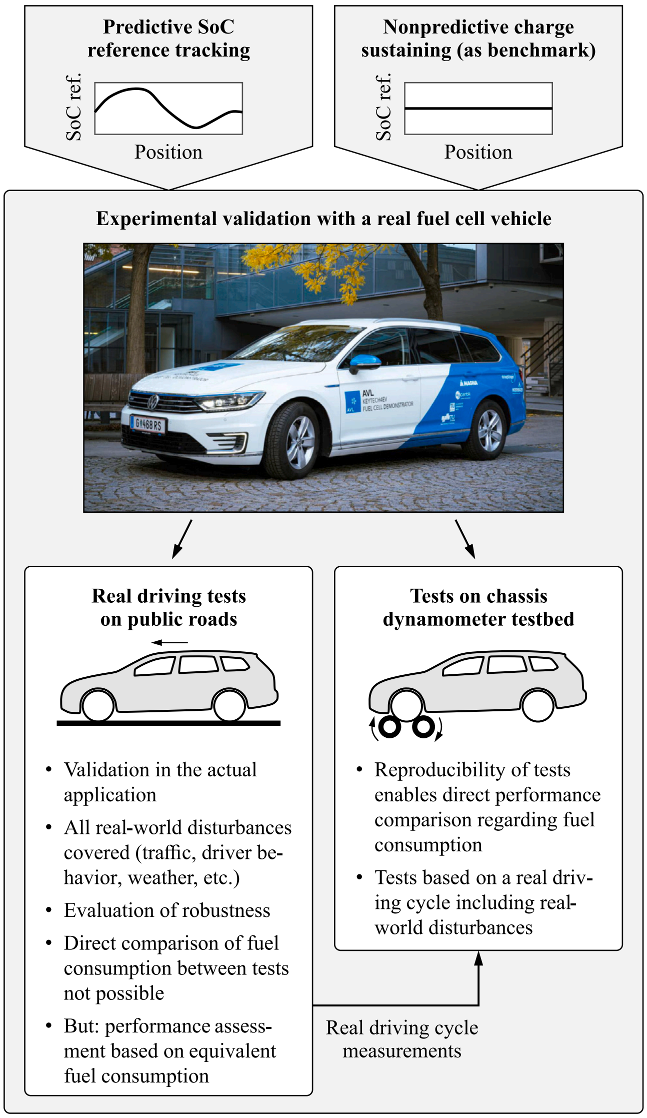

(a) Illustration of the experimental validation with a fuel cell demonstrator vehicle of AVL List GmbH.

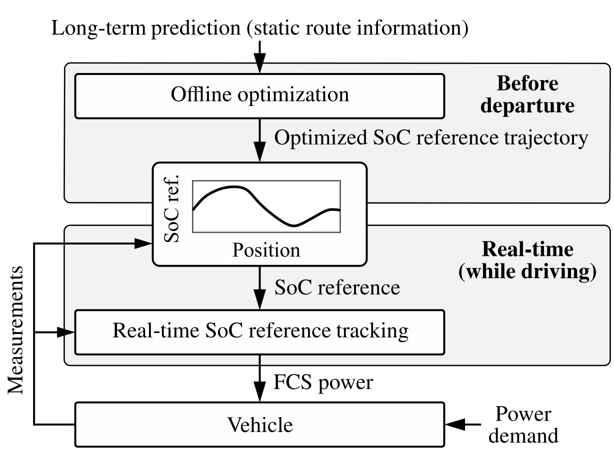

(b) Route-informed predictive SoC reference tracking.

Fig. 2. Experimental validation of predictive SoC reference tracking.

Table 1
Model parameters of the demonstrator vehicle.

Vehicle dynamics model	
Vehicle mass, m (kg)	1950
Frontal area, A_f (m^2)	2.12
Air density, ρ (kg m^{-3})	1.204
Aerodynamic drag coefficient, c_d	0.346
Rolling friction coefficient, c_r	0.0055
Traction motor efficiency, η_m	0.87
Auxiliary power demand (estimate), P_{aux} (kW)	1
Powertrain model	
FCS idle power, P_{FCS}^{idle} (kW)	8
Max. FCS power, P_{FCS}^{max} (kW)	50
Battery energy capacity (kWh)	9.9
Battery capacity, Q_{nom} (A h)	28.28
Internal resistance, R_{int} (Ω)	0.15
Min. battery power (continuous), P_b^{min} (kW)	−20
Max. battery power (continuous), P_b^{max} (kW)	30
Min. SoC, ξ^{min}	0.2
Max. SoC, ξ^{max}	0.8

The investigated predictive EMS derives a long-term power demand prediction for a planned driving mission from easily available static route information, i.e., the altitude profile and legal speed limits. Based on the long-term prediction and a control-oriented vehicle model, a distance-based reference trajectory for the battery SoC is optimized before departure (see Fig. 2(b)). While driving, a simple real-time controller tracks the optimized SoC reference trajectory to determine the real-time power split between the FCS and the battery. The simple real-time EMS is chosen for the validation to assess the baseline for performance improvements by considering route-based power demand predictions, which might even be exceeded with more advanced methods. Moreover, the low computational complexity and robustness of the investigated EMS make it an interesting candidate for an immediate industrial application. To ensure a fair comparison, the nonpredictive charge sustaining strategy used as a benchmark is based on the same tracking controller as the proposed predictive SoC reference tracking but considers a constant SoC reference.

The remainder of this article is structured as follows. First, the fuel cell vehicle used for the validation and the control-oriented vehicle modeling are described in Section 2. Then, the predictive SoC reference tracking strategy is introduced in Section 3. In Section 4, the computation of the equivalent fuel consumption is described, which is the basis for the quantitative evaluation of the fuel efficiency. The experimental validation of the predictive SoC reference tracking based on real driving tests and dynamometer tests is presented in Section 5. A conclusion in Section 6 finalizes this article.

2. Fuel cell vehicle and control-oriented modeling

The predictive EMS investigated in this work is evaluated and compared with the nonpredictive strategy in experiments with a fuel cell demonstrator vehicle of AVL List GmbH. The demonstrator vehicle, which is shown in Fig. 2(a), is based on a Volkswagen Passat GTE and equipped with an FCS with a nominal power of 50 kW and a battery with a nominal energy capacity of 9.9 kWh.

To conduct the offline optimization of the SoC reference trajectory before departure, appropriate models of the vehicle components are required. First, a model of the vehicle longitudinal dynamics is used to derive a prediction of the power demand for the entire driving mission from static route information, i.e., the altitude profile and legal speed limits. Second, a model of the hybrid powertrain is used to optimize the energy management for the predicted power demand. To keep the computational complexity of the offline optimization low, simplified and control-oriented models are used. Nevertheless, the simplified modeling does not affect the performance of the predictive concept because the accuracy of the long-term power demand prediction is limited in any case. In the following, the vehicle dynamics model is described first before the powertrain model is introduced.

2.1. Vehicle dynamics for power demand prediction

To estimate the power demand for the entire driving mission based on the speed limits and the altitude profile along the route, a model of the longitudinal vehicle dynamics is used. The model considers the traction force, aerodynamic drag, rolling resistance, and the gravitational force

$$m\frac{\mathrm{d}v}{\mathrm{d}t} = \eta_{\mathrm{m}}^{\operatorname{sgn} P_{\mathrm{tr}}}\frac{P_{\mathrm{tr}}}{v} - \frac{\rho A_{\mathrm{f}} c_{\mathrm{d}}}{2}v^2 - c_{\mathrm{r}} mg\cos\theta - mg\sin\theta \tag{1}$$

where m denotes the vehicle mass, v the velocity, t the time, η_{m} the traction motor efficiency, P_{tr} the traction motor power, ρ the air density, A_{f} the frontal area of the vehicle, c_{d} the aerodynamic drag coefficient, c_{r} the rolling friction coefficient, g the gravitational acceleration, and θ the road inclination angle, which can be derived from the altitude profile. The parameters are assumed to be known and summarized in the upper part of Table 1. Based on the model of the longitudinal vehicle dynamics, a prediction of the traction motor power can be derived from the speed limits and the inclination angle along the route. Here, system power constraints are considered to prevent infeasible power demands during velocity transients and uphill sections. Additionally, the vehicle velocity is saturated depending on the road curvature to prevent infeasible cornering speeds, which improves the prediction quality particularly in urban and mountainous areas.

The prediction of the overall electric power demand P_{el} can then be computed with

$$P_{\mathrm{el}} = P_{\mathrm{tr}} + P_{\mathrm{aux}} \tag{2}$$

where P_{aux} denotes the power demand of the auxiliary systems. The variation of the auxiliary power demand is hardly predictable over long-term prediction horizons, and its magnitude is relatively small compared to the traction power demand. Therefore, a constant estimate of the auxiliary power demand serves as a sufficient approximation for the prediction. The prediction of the overall power demand is the input for the offline optimization of the energy management before departure.

2.2. Powertrain model for offline optimization

The offline optimization of the SoC reference trajectory before departure is based on a model of the powertrain, which consists of the FCS and the battery (see Fig. 1). The sum of the FCS power P_{FCS} and battery power P_{b} satisfies the overall electric power demand

$$P_{\mathrm{el}} = P_{\mathrm{FCS}} + P_{\mathrm{b}} \tag{3}$$

whereby the power split between the two power sources is determined by the EMS and, therefore, the variable to be optimized. To provide the optimized SoC reference trajectory for the real-time energy management shortly after the route was determined, the offline optimization must be fast, i.e., its computational complexity must be low. Therefore, the two power sources are described with simplified, quasistatic models focusing on the characteristics relevant for the long-term optimization. Note that a consideration of more detailed power source dynamics would not necessarily improve the overall performance because the accuracy of the long-term prediction is limited and certain deviations due to real-world influences are expected.

The FCS is considered with a quadratic polynomial model describing the fuel consumption rate $\dot{m}_{\mathrm{FCS}}(P_{\mathrm{FCS}})$ as a function of the FCS power, where the compressor power demand is implicitly taken into account. In this study, the fuel consumption curve was identified based on tank measurements, which include purging losses, considering measurements of several real-world driving missions. The fuel consumption

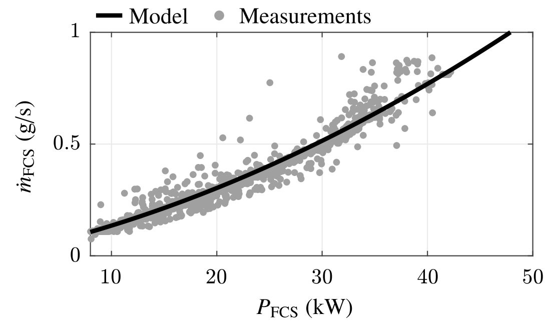

(a) Fuel consumption curve of the FCS. The $\dot{m}_{\mathrm{FCS}}$ measurements are estimated based on the measured current.

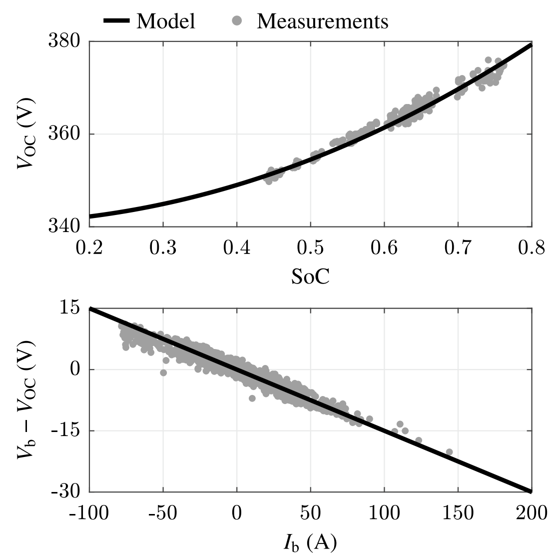

(b) Equivalent circuit model of the battery. The V_{OC} measurements in the upper plot are approximated with the measured battery voltage under small loads.

Fig. 3. Identified FCS model and battery model compared to sets of measurements.

curve is compared to a set of measurements in Fig. 3(a). The measurements deviate from the model within a certain range due to the neglected system dynamics and other influences. However, the model sufficiently describes the characteristic of the fuel consumption rate for the offline optimization based on the long-term prediction. To mitigate FCS degradation, the FCS is only operated between the idle power limit $P_{\mathrm{FCS}}^{\mathrm{idle}}$ and the maximum power limit $P_{\mathrm{FCS}}^{\mathrm{max}}$ when active. If the power request is low, the EMS can put the FCS into a stopmode where the fuel consumption rate is zero but FCS-related auxiliaries including the compressor remain active. Because the auxiliaries are not shut down, frequent switching between active operation and stopmode is possible without restrictions. The FCS power in stopmode is assumed to be zero, i.e., the electric load of the auxiliaries is neglected.

The battery behavior is approximated with an equivalent circuit model considering ohmic losses where the battery voltage V_{b} linearly depends on the battery current I_{b}:

$$V_{\mathrm{b}} = V_{\mathrm{OC}}(\xi) - R_{\mathrm{int}} I_{\mathrm{b}}. \tag{4}$$

Here, the open-circuit voltage V_{OC} varies depending on the battery SoC ξ, which is described with a quadratic polynomial, whereas the ohmic resistance R_{int} is assumed constant. In this study, the battery model was identified based on battery voltage and current measurements of several real-world driving missions. Despite the simplification, the battery fits the measurements well, as shown in Fig. 3(b). With the equivalent circuit model, the dynamics of the battery SoC can be described as a nonlinear function of the battery power P_b with

$$\dot{\xi} = -\frac{V_\mathrm{OC} - \sqrt{V_\mathrm{OC}^2 - 4P_\mathrm{b}R_\mathrm{int}}}{2Q_\mathrm{nom}R_\mathrm{int}} \tag{5}$$

where the battery capacity Q_nom is assumed to be known. The powertrain model parameters of the demonstrator vehicle are summarized in the lower part of Table 1.

3. Predictive SoC reference tracking

The goal of the predictive EMS is to improve the fuel efficiency and ensure feasible operation by considering a long-term prediction of the driving mission that is based on easily available static route information, i.e., the altitude profile and legal speed limits. Therefore, the basic assumptions of the predictive approach are that the route is determined before departure and the mentioned static route information is accessible, e.g., through map services or the onboard navigation system. Although this kind of prediction has limited accuracy, it has shown to be highly effective for optimizing the energy management because it covers the entire driving mission and, thus, provides the long prediction horizon necessary to actively involve the battery in the energy management. Moreover, the route-based prediction is available before departure so that the predictive EMS can be divided into two stages (see Fig. 2(b)):

1. In the *offline optimization* before departure, the energy management is optimized based on the long-term power demand prediction, yielding an optimized, distance-based SoC reference trajectory. The optimization can be conducted either onboard, if the required computational resources are available, or on a cloud computing server.
2. The onboard *real-time energy management* determines the setpoint for the FCS power by tracking the optimized SoC reference trajectory considering the actual power demand and system constraints.

The significant advantage of the two-stage approach is that the real-time control can be realized with a computationally simple tracking controller because the predictive information is already processed before departure. In the following, the two stages are described in more detail.

3.1. Offline optimization before departure

To optimize the SoC reference trajectory for the planned driving mission before departure, a long-term power demand prediction is needed. The power demand prediction is derived from the altitude profile and speed limits along the route based on the vehicle dynamics model as described in Section 2.1. Due to the limited accuracy of the long-term prediction, a relatively rough discretization interval can be chosen for the offline optimization, which allows for a considerable acceleration of the optimization without affecting the overall performance of the predictive EMS. For this purpose, the power demand prediction is segmented with

$$P_{\mathrm{el},l} = \frac{\int_{t_l}^{t_{l+1}} P_\mathrm{el}\,\mathrm{d}t}{\Delta t_l} \tag{6}$$

for all $l = 1\ldots(L-1)$ before the offline optimization, where Δt_l denotes the time spent in the lth segment and $(L-1)$ is the number of segments.

The objective is to minimize the fuel consumption, which is specified in discrete-time form assuming a zero-order hold for the power demand, the FCS power, and the battery power

$$\begin{aligned} \min J = \sum_{l=1}^{L-1} \dot{m}_\mathrm{FCS}(P_{\mathrm{FCS},l})\Delta t_l \\ \text{s.t.} \quad & \xi_1 = \xi_\mathrm{init} \\ & \xi_L \geq \xi_\mathrm{end} \\ & \xi^\mathrm{min} \leq \xi_l \leq \xi^\mathrm{max} \\ & P_\mathrm{b}^\mathrm{min} \leq P_{\mathrm{b},l} \leq P_\mathrm{b}^\mathrm{max} \\ & P_{\mathrm{FCS},l} \in \mathcal{U} \end{aligned} \tag{7}$$

where the feasible FCS power range $\mathcal{U}$ includes the stopmode

$$\mathcal{U} = \left\{ P \in \mathbb{R} : P_\mathrm{FCS}^\mathrm{idle} \leq P \leq P_\mathrm{FCS}^\mathrm{max} \vee P = 0\,\mathrm{W} \right\} \tag{8}$$

and ξ_init denotes the initial SoC, ξ_end the minimum SoC at the end of the driving mission, ξ^min the minimum SoC, and ξ^max the maximum SoC. The minimum battery power $P_\mathrm{b}^\mathrm{min}$ and maximum battery power $P_\mathrm{b}^\mathrm{max}$ are chosen conservatively according to the continuous charging and discharging current specifications of the battery to ensure feasibility of the SoC reference.

In this study, the optimal control problem is solved with dynamic programming (DP), which is a dynamic optimization method [46]. The significant advantage of DP over methods based on Pontryagin's minimum principle, a common alternative for solving optimal energy management problems, is that all specified constraints including the SoC constraints can be considered directly. Thanks to the simplified powertrain modeling, the problem includes only one state (ξ) and one control input (P_FCS). Together with the rough discretization intervals, the low dimension of the problem results in a low computational complexity, which ensures that the optimization results can be provided shortly after the route was determined. More details regarding the DP implementation for the present problem can be found in the literature, e.g., [20,23].

The output of the offline optimization is the optimized SoC reference trajectory. To limit the effects of unpredicted velocity deviations and vehicle standstills on the predictive energy management, the SoC reference trajectory $\xi^\mathrm{ref}(s)$ is specified in the distance-domain, i.e., as function of the position s along the route and not as a function of time. Consequently, unpredicted variations in the driving time that have occurred in the past do not affect the optimality of the SoC reference trajectory for the trip remainder.

3.2. Real-time SoC reference tracking

The real-time EMS determines the FCS power setpoint based on a computationally simple controller that tracks the optimized reference trajectory while driving. The position along the driving mission, which is required to access the current SoC reference value, is determined by measuring the covered distance. In this study, the real-time SoC reference tracking strategy extends an already implemented nonpredictive charge sustaining controller with a PI controller considering the deviation from the optimized SoC reference $\Delta\xi = (\xi^\mathrm{ref}(s) - \xi)$ at the current position:

$$P_\mathrm{FCS}^\mathrm{track} = k_\mathrm{P}\Delta\xi + k_\mathrm{I}\int_0^t \Delta\xi\,\mathrm{d}\tau + P_\mathrm{FCS}^\mathrm{NP}(P_\mathrm{el}, \xi). \tag{9}$$

Here, $P_\mathrm{FCS}^\mathrm{track}$ denotes the FCS power according to the tracking controller and $P_\mathrm{FCS}^\mathrm{NP}(P_\mathrm{el}, \xi)$ the nonpredictive component, which is described by a 2-D map depending on the measured power demand and SoC. The nonpredictive component, which was tuned and tested based on expert knowledge, is included to ensure reliable operation where the power demand is robustly satisfied within reasonable time in any situation. Because the SoC reference is optimized based on the power demand prediction, which is expected to deviate from the actual power demand to some extent, the PI controller gains k_P and k_I are chosen such that certain freedom for deviation from the SoC reference is provided to adapt to the unpredicted disturbances.

To prevent infeasible power requests from the FCS, the FCS power resulting from the tracking controller is saturated within the feasible power range determined by the constraints on the FCS power, FCS power increments, and battery power, which yields the FCS power setpoint $P_{\mathrm{FCS}}^{\mathrm{setp}}$:

$$\begin{aligned} P_{\mathrm{FCS}}^{\mathrm{setp}} = \min_{P_{\mathrm{FCS}}} & \left| P_{\mathrm{FCS}}^{\mathrm{track}} - P_{\mathrm{FCS}} \right| + q_s s \\ \text{s.t.} \quad & 0\,\mathrm{W} \leq P_{\mathrm{FCS}} \leq P_{\mathrm{FCS}}^{\max} \\ & \Delta P_{\mathrm{FCS}}^{\min} \leq P_{\mathrm{FCS}} - P_{\mathrm{FCS}}^{\mathrm{prev}} \leq \Delta P_{\mathrm{FCS}}^{\max} \\ & \bar{P}_{\mathrm{b}}^{\min} - s \leq P_{\mathrm{el}} - P_{\mathrm{FCS}} \leq \bar{P}_{\mathrm{b}}^{\max} + s. \end{aligned} \tag{10}$$

Here, $P_{\mathrm{FCS}}^{\mathrm{prev}}$ denotes the FCS power in the previous instance, and $\Delta P_{\mathrm{FCS}}^{\min}$ and $\Delta P_{\mathrm{FCS}}^{\max}$ are the minimum and maximum FCS power increments per time step, respectively. The battery power constraints $\bar{P}_{\mathrm{b}}^{\min}$ and $\bar{P}_{\mathrm{b}}^{\max}$ adapt according to the battery management system in real time and are considered as soft constraints to avoid infeasibility. For this purpose, a slack variable $s \geq 0$ and a weighting coefficient $q_s > 1$ are used. Note that the problem in Eq. (10) can be solved efficiently with a series of logical operations, see [3]. The constraints on the battery SoC are implicitly considered by tracking the optimized SoC reference trajectory.

If the resulting FCS power setpoint is considerably lower than the idle power limit, the real-time EMS puts the FCS into the stopmode where the fuel supply is stopped:

$$P_{\mathrm{FCS}} = \begin{cases} \min(P_{\mathrm{FCS}}^{\mathrm{setp}}, P_{\mathrm{FCS}}^{\mathrm{idle}}), & \text{if } P_{\mathrm{FCS}}^{\mathrm{setp}} \geq P_{\mathrm{FCS}}^{\mathrm{thr}} \\ 0\,\mathrm{W}, & \text{otherwise.} \end{cases} \tag{11}$$

Here, the power threshold $P_{\mathrm{FCS}}^{\mathrm{thr}}$ is a tuning parameter. Because FCS-related auxiliaries such as the compressor remain active in stopmode, a fast switch to active operation is possible at any time.

4. Evaluation of fuel consumption

The predictive SoC reference tracking is compared with a nonpredictive method in experiments with the real fuel cell vehicle in Section 5. The experiments include real driving tests on public roads, where variations in the power demand are inevitable due to numerous real-world influences, such as traffic, driver behavior, and weather. But also in the subsequently conducted dynamometer tests, the power demand varies within certain tolerances. Moreover, the final battery SoC generally differs from the initial SoC depending on the power demand profile because both EMSs must ensure freedom for deviation from the SoC reference to adapt to unpredicted disturbances. Consequently, the net energy contribution of the battery varies between different tests.

To allow for a performance comparison despite these variations, the experimental results are evaluated based on the equivalent fuel consumption m_{eq} that takes into account corrections for variations in the battery energy contribution Δm_{b} and the traction motor energy Δm_{tr}:

$$m_{\mathrm{eq}}(t) = m_{\mathrm{H_2}}(t) + \Delta m_{\mathrm{b}}(t) + \Delta m_{\mathrm{tr}}(t). \tag{12}$$

Here, the actual fuel consumption $m_{\mathrm{H_2}}$ is computed based on tank measurements and, thus, includes purging losses.

The correction for the battery energy is based on the deviation of the SoC from the initial SoC considering the open-circuit voltage model

$$\Delta m_{\mathrm{b}}(t) = -\frac{Q_{\mathrm{nom}}}{H_{\mathrm{i}} \bar{\eta}_{\mathrm{FCS}}} \int_{\xi_{\mathrm{init}}}^{\xi(t)} V_{\mathrm{OC}}(\xi)\,\mathrm{d}\xi \tag{13}$$

where $H_{\mathrm{i}} = 120\,\mathrm{MJ\,kg^{-1}}$ denotes the lower heating value of hydrogen. The mean FCS efficiency

$$\bar{\eta}_{\mathrm{FCS}} = \frac{\int_0^{t_{\mathrm{end}}} P_{\mathrm{FCS}}\,\mathrm{d}t}{H_{\mathrm{i}} m_{\mathrm{H_2}}} \tag{14}$$

is computed individually for each test because it strongly varies depending on the EMS.

The power demand correction takes into account variations in the traction motor power with respect to a reference test. Variations in the power demand of the auxiliaries are not considered because they depend on the EMS. This means that, for example, an increased fuel consumption due to higher cooling power demands is *not* corrected. For the dynamometer tests, where the driving times are identical, the power demand correction can be evaluated continuously over time with

$$\Delta m_{\mathrm{tr}}(t) = \frac{\int_0^t P_{\mathrm{tr}}(\tau) - P_{\mathrm{tr,ref}}(\tau)\,\mathrm{d}\tau}{H_{\mathrm{i}} \bar{\eta}_{\mathrm{FCS}}} \tag{15}$$

where $P_{\mathrm{tr,ref}}$ denotes the traction motor power of the reference test. For the real driving tests, the driving time varies depending on traffic. Therefore, the correction is only computed for the entire test with

$$\Delta m_{\mathrm{tr}} = \frac{E_{\mathrm{tr}} - E_{\mathrm{tr,ref}}}{H_{\mathrm{i}} \bar{\eta}_{\mathrm{FCS}}} \tag{16}$$

where E_{tr} and $E_{\mathrm{tr,ref}}$ denote the traction energies of the entire test and reference test, respectively.

5. Experimental results

The predictive SoC reference tracking is evaluated and compared with a nonpredictive EMS in experiments with the real fuel cell passenger vehicle. The nonpredictive EMS is a charge sustaining strategy that maintains the SoC around a constant reference value of 0.6. The nonpredictive charge sustaining is based on the same real-time tracking controller as the predictive SoC reference tracking, which allows for a fair evaluation of the fuel efficiency gains by considering route-based long-term predictions.

To ensure an application-oriented validation of the predictive EMS, the experimental evaluation puts a strong emphasis on real-world driving. Unlike synthetic driving cycles, real-world driving is affected by various random influences, such as traffic, traffic regulation, driver behavior, and weather, which cause considerable deviations from the long-term velocity prediction including vehicle standstills with varying standstill times. The experimental validation is based on two types of tests:

- *Real driving tests* were conducted on predetermined routes on public roads including urban, rural, and freeway driving. These tests are influenced by varying traffic conditions and vehicle standstills, which have an impact on the total driving time. The tests are therefore particularly interesting for analyzing the robustness of the predictive EMS against unpredicted disturbances in the real-world application.
- *Dynamometer tests* were carried out based on a *selected real driving cycle* on a chassis dynamometer testbed. In contrast to the real driving tests conducted on public roads, traction power demand profiles can be reproduced multiple times on the dynamometer testbed, which enables a direct comparison between the two EMSs and drawing more significant conclusions regarding the benefit of the predictive EMS on the fuel efficiency. Also in the dynamometer tests, the real driving cycle covers real-world disturbances including vehicle standstills, which are not considered in the speed limit-based prediction. In addition, dynamometer tests based on the "Worldwide Harmonized Light-Duty Vehicles Test Cycle" (WLTC), a standard cycle widely used in the literature, were conducted.

All tests started and ended with an SoC close to 0.6, and the small differences between the initial and the final SoC are considered in the quantitative evaluation based on the equivalent fuel consumption as described in Section 4.

The predictive strategy considers route-based predictive information, i.e., the altitude profile along the route and a speed limit-based prediction of the velocity, to conduct the offline optimization before departure. In this work, both pieces of information were obtained from *AVL Route Studio*, a test cycle preparation tool. The tool considers longitudinal vehicle dynamics during transients and limits the velocity depending on the road curvature. In this way, feasible long-term velocity predictions can be generated conveniently for testing purposes.

In the following, the real driving tests are presented first, focusing on quantitative results. Then, the dynamometer tests are discussed, where the qualitative differences in the energy management of the two EMSs are analyzed in addition to a quantitative evaluation.

5.1. Real driving tests

The real driving tests were conducted on two different routes on public roads, which are labeled "route A" and "route B" in the following. The two routes represent day-to-day driving missions such as commuting and include shares of urban, rural, and freeway driving. On both predetermined routes, tests were repeated several times with the predictive SoC reference tracking and the nonpredictive charge sustaining. The covered distance, the altitude profile, the speed limits, and the speed limit-based prediction of the individual tests on a route are identical, whereas the velocity profile and, thus, the power demand profile and the total driving time vary because of real-world influences, such as traffic, traffic regulation, driver behavior, and weather. These influences also cause vehicle standstills with varying standstill times. The primary objective of the real driving tests is the experimental validation of the robustness of the predictive SoC reference tracking in the actual application, where unpredicted disturbances caused by the real-world influences are inevitable. For this purpose, the performance advantage over the nonpredictive EMS is assessed based on the equivalent fuel consumption. Moreover, the quality of the long-term velocity predictions is assessed with plots comparing the measured and predicted velocity profiles over distance. The distance-based plots do not reflect the effects of velocity deviations on the driving time, which is meaningful for the assessment because the predictive EMS compensates for these effects by using a distance-based SoC reference trajectory.

5.1.1. Real driving tests on route A

Route A has a length of 26 km and includes rural and urban roads. The altitude profile and the speed limit-based velocity prediction of route A are shown in Figs. 4(a) and 4(b), respectively. Based on this information, the long-term power demand prediction for the driving mission was derived, and the energy management was optimized (also see Fig. 4(a)). The optimized SoC trajectory, which is used as reference for the predictive SoC reference tracking, plans that the battery supports the FCS in the high-power uphill section and is recharged in the subsequent downhill section. In this way, the FCS is operated close to the idle power limit, where the FCS efficiency peaks, unless the power demand significantly exceeds the maximum continuous battery power limit of 30 kW.

Seven real driving tests, which are labeled A1 to A7, were performed on route A. Their measured velocity signals are compared to the long-term velocity prediction in Fig. 4(b). The speed limit-based prediction provides a good estimate but inevitably deviates because of traffic influences, particularly in the final urban part, where several stops were required.

To evaluate the potential of the predictive EMS under these varying disturbances, the route was driven twice with the nonpredictive charge sustaining (tests A1 and A2) and five times with the predictive SoC reference tracking (tests A3 to A7). The quantitative results are presented in Table 2a and 2b. The strong influence of traffic is reflected in the cumulated standstill time, which varies between 3.7 and 12.2 min and affects the total driving time. The fuel efficiency of the individual tests is evaluated based on the equivalent fuel consumption, which takes into account corrections for deviations in the traction energy and the final

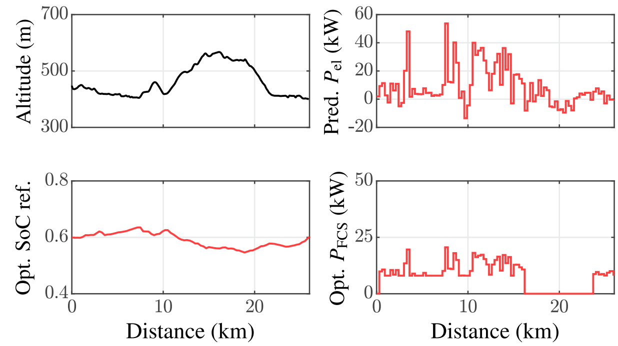

(a) Altitude profile and long-term prediction of the electric power demand of route A (upper plots) and the results of the offline optimization: optimized SoC reference trajectory and the corresponding FCS power (lower plots).

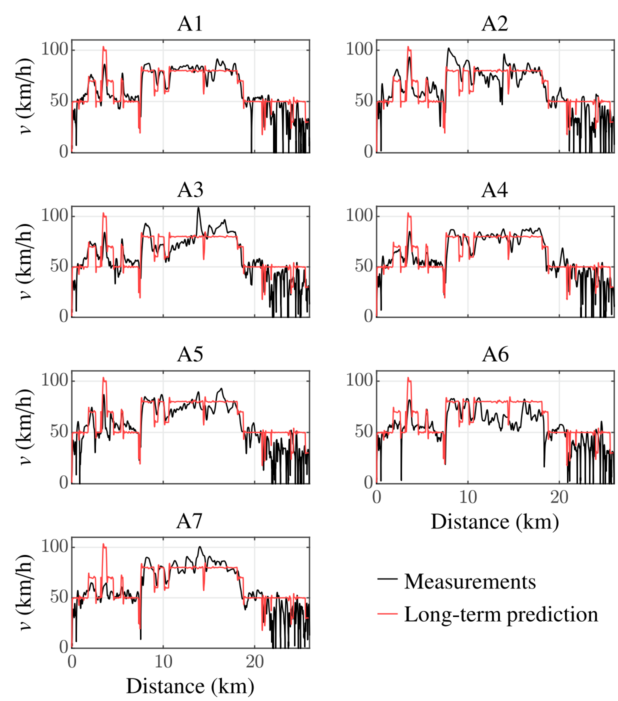

(b) Velocity measurements of the seven real driving tests compared to the speed limit-based velocity prediction of route A.

Fig. 4. Real driving tests on route A.

SoC. The two tests that applied the nonpredictive charge sustaining strategy (tests A1 and A2) showed an identical performance with an equivalent fuel consumption of 0.242 kg. Compared to this result, all tests using the predictive SoC reference tracking showed a reduced equivalent fuel consumption with improvements ranging from 0.4 % to 7.4 %. On average, the predictive SoC reference tracking yielded a considerable improvement of 4.6 %. The measurements indicate that this improvement results from an increase in the mean FCS efficiency thanks to the predictive information. Regarding the effect of the EMS on ohmic battery losses, no clear statement is possible. Feasible operation was ensured, i.e., the power demand was satisfied without violating powertrain constraints, in all tests.

Remarkably, the considerable improvements in the fuel efficiency were achieved with a rather small amplitude in the SoC reference trajectory for this route. This indicates that the results could also be achieved with a considerably smaller battery capacity.

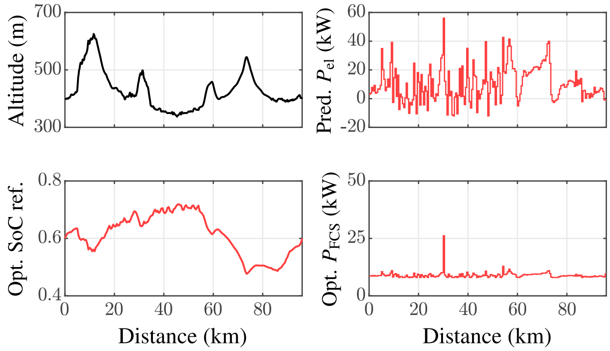

(a) Altitude profile and long-term prediction of the electric power demand of route B (upper plots) and the results of the offline optimization: optimized SoC reference trajectory and the corresponding FCS power (lower plots).

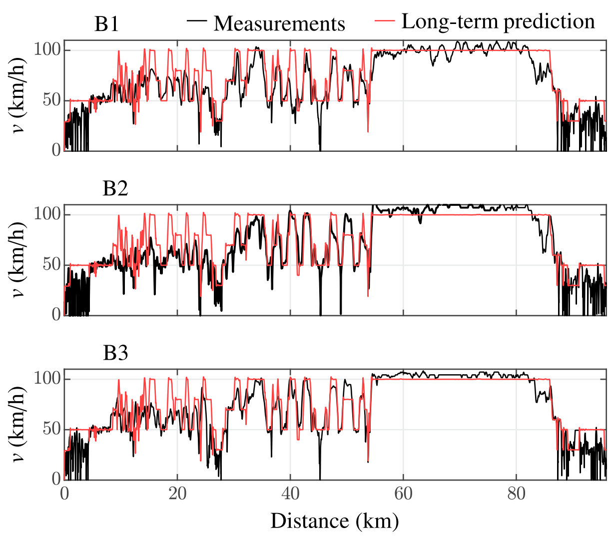

(b) Velocity measurements of the three real driving tests compared to the speed limit-based velocity prediction of route B.

Fig. 5. Real driving tests on route B.

5.1.2. *Real driving tests on route B*

Three tests were conducted on route B, which has a length of 96 km and covers urban, rural, and freeway driving. The route-based long-term prediction, the results of the prediction-based offline optimization, and the comparison between the predicted and the measured velocities of the three tests are shown in Fig. 5. Again, the long-term velocity prediction gives a good estimate but shows traffic-induced deviations, particularly in the urban parts of the route. Similar to the optimization outcome for route A, the optimal energy management for the predicted power demand plans a rather steady operation of the FCS in the low-power range, where the FCS efficiency is high. Consequently, most of the dynamic share of the predicted power demand is covered by the battery, which can be seen in optimized SoC profile. Due to the longer distance and the higher changes in altitude compared to route A, the optimized SoC profile shows a considerably higher amplitude here.

The first test (B1) was performed with the nonpredictive charge sustaining, and the other two tests (B2 and B3) applied the predictive SoC reference tracking. The results are presented in Table 2c. Both B2 and B3 show a considerable reduction in the equivalent fuel consumption with respect to the test applying the nonpredictive EMS with improvements of 5.4 % and 3.6 %, respectively. On average, the equivalent fuel consumption was reduced by 4.5 %. The predictive strategy caused an increase in the ohmic battery losses due to the enhanced battery use. However, the mean FCS efficiency was improved significantly from 51.4 % for the nonpredictive EMS to 55 % for the predictive strategy, which overcompensated for the increased battery losses and resulted in the significantly higher fuel efficiency. Also, feasible operation was ensured in all tests.

Table 2
Results of the real driving tests comparing the two EMSs: nonpredictive charge sustaining (CS) vs. predictive SoC reference tracking (SoC RT).

(a) Real driving tests on route A.

	A1	A2	A3	A4
EMS	**CS**	**CS**	**SoC RT**	**SoC RT**
Traction energy (kWh)	3.44	3.42	3.28	3.32
Total driving time (min)	36.7	43.5	35.8	35.3
Standstill time (min)	4.7	12.2	3.7	4.4
m_{eq} **(kg)**	**0.242**	**0.242**	**0.228**	**0.23**
Relative difference	**0%**	**0%**	**−5.8%**	**−5%**
Mean FCS efficiency	49.1%	49.5%	51.7%	50.8%
Battery losses (kWh)	0.061	0.088	0.069	0.046

(b) Real driving tests on route A (continuation).

	A5	A6	A7
EMS	**SoC RT**	**SoC RT**	**SoC RT**
Traction energy (kWh)	3.2	3.31	3.38
Total driving time (min)	38.7	39.8	39.1
Standstill time (min)	4.7	5.3	6.7
m_{eq} **(kg)**	**0.224**	**0.231**	**0.241**
Relative difference	**−7.4%**	**−4.5%**	**−0.4%**
Mean FCS efficiency	52.4%	51.4%	50.4%
Battery losses (kWh)	0.057	0.044	0.057

(c) Real driving tests on route B.

	B1	B2	B3
EMS	**CS**	**SoC RT**	**SoC RT**
Traction energy (kWh)	12.09	13.88	11.96
Total driving time (min)	120.7	120.8	112.4
Standstill time (min)	13.8	13.7	8.5
m_{eq} **(kg)**	**0.811**	**0.767**	**0.782**
Relative difference	**0%**	**−5.4%**	**−3.6%**
Mean FCS efficiency	51.4%	55%	55%
Battery losses (kWh)	0.163	0.262	0.25

5.1.3. *Summary of real driving tests*

The evaluation based on the equivalent fuel consumption validated the robustness of the predictive SoC reference tracking for the real-world application. Even though the tests were affected by considerable disturbances with respect to the speed limit-based long-term prediction, the results of the real driving tests indicate that the predictive SoC reference tracking performs significantly better than the nonpredictive charge sustaining with average reductions in the equivalent fuel consumption of 4.6 % on route A and 4.5 % on route B. The analysis of the results also indicates that the improved fuel economy is achieved by an increase in the mean FCS efficiency, whereas influences of ohmic battery losses are less relevant.

However, the variances in the velocity and power demand profiles and the standstill times of the real driving tests do not allow for a direct comparison between the predictive SoC reference tracking and the nonpredictive charge sustaining. Therefore, dynamometer tests were conducted based on a selected real driving cycle, which are presented in the following.

5.2. Dynamometer tests

To draw more significant conclusions regarding improvements in the fuel efficiency and compare the two EMSs also qualitatively, tests were performed on the chassis dynamometer testbed, where velocity and traction power profiles can be reproduced within certain tolerances. The dynamometer tests are based on the velocity measurements of a selected real driving cycle, namely B3. Therefore, the dynamometer tests cover the significant disturbances with respect to the speed limit-based prediction that were experienced in the corresponding real driving test including vehicle standstills. Moreover, the chassis dynamometer tests involve the entire vehicle, and thus, influences of the auxiliary systems and the drivetrain are also included. In addition to the dynamometer tests based on the real driving cycle, tests based on the standard WLTC were conducted. The results are described below.

5.2.1. Dynamometer tests based on the real driving cycle

The altitude profile, velocity profile, and traction power profile of the real driving cycle B3 are shown in Fig. 6(a). The driving cycle covers urban, rural, and freeway driving and includes substantial changes in altitude, which dominate the traction power profile. The influence of the altitude profile on the traction power is particularly evident on the freeway section between 55 km and 85 km. Besides measurements, Fig. 6(a) also includes the speed limit-based velocity prediction, which considers the vehicle dynamics during transients and limits the velocity depending on the road curvature. As already discussed for the real driving tests, the long-term velocity prediction gives a good estimate of the actual velocity but inevitably deviates due to real-world influences. Particularly in the urban parts at the beginning and the end of the driving cycle, the actual velocity is affected by numerous unpredicted vehicle stops and dense traffic. Nevertheless, the long-term traction power prediction, which is derived from the predicted velocity and the altitude profile, provides a good estimate of the measured power demand except for fast dynamics, i.e., spikes in the measured traction power, which are strongly influenced by the unpredicted disturbances. Based on the power demand prediction, the energy management was optimized.

The result of the offline optimization and the comparison of the predictive SoC reference tracking and the nonpredictive charge sustaining are shown in Fig. 6(b). The optimal energy management regarding the prediction aims at operating the FCS closely to the idle power limit, where the FCS efficiency peaks, but also shows a slight power-following behavior, which reduces ohmic battery losses. Consequently, the optimized SoC reference is clearly influenced by the changes in altitude and the implicated variations in the traction power. The optimized SoC reference basically plans to charge the battery in the low-power sections of the driving cycle, e.g., during descents, and discharge the battery in the high-power sections, e.g., in the uphill freeway section starting at 55 km.

Not considering this predictive information, the charge sustaining strategy maintains the SoC around a constant reference of 0.6. Although the controller provides certain freedom for deviation from the constant reference, the charge sustaining strategy shows a clear power-following behavior, i.e., the FCS power follows the power demand. Thus, the FCS is operated in the low-power range frequently entering the stopmode in the low-power sections of the cycle and must satisfy high power requests during the high-power sections, particularly in the uphill freeway section starting at 55 km.

Unlike the charge sustaining strategy, the predictive SoC reference tracking strategy tracks the optimized SoC reference trajectory. Even though the measured FCS power of the predictive SoC reference tracking deviates from the offline solution due to the unpredicted real-world influences, the SoC follows the reference trajectory adequately. Compared to the nonpredictive strategy, the predictive SoC reference tracking requests more power from the FCS in the low-power sections of the cycle and charges the battery in this way. In return, the battery

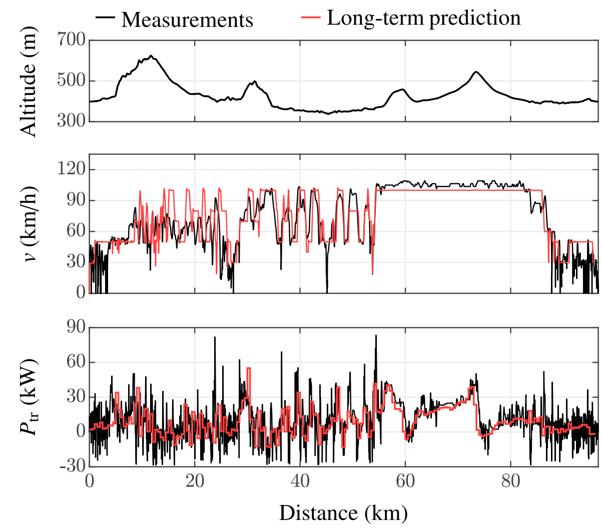

(a) Altitude, velocity, and traction motor power of the real driving cycle compared to the speed limit-based prediction.

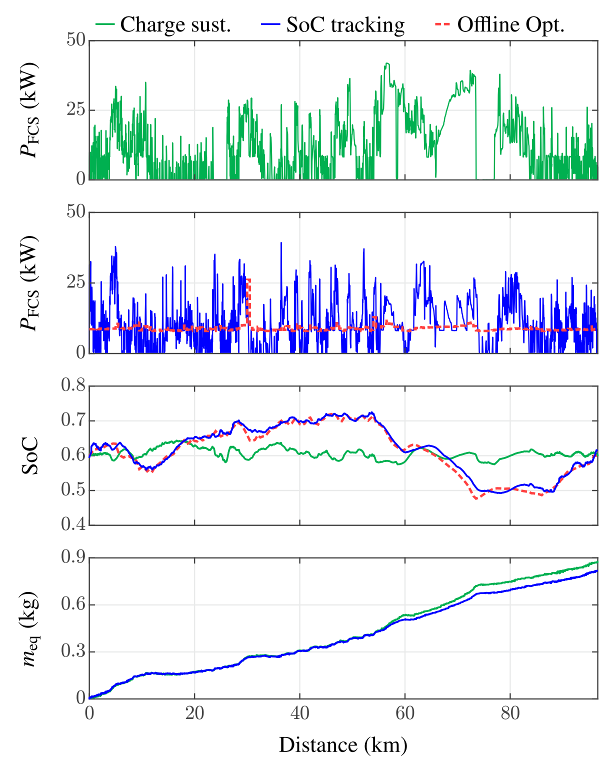

(b) Comparison of the nonpredictive charge sustaining strategy and the predictive SoC reference tracking. Additionally, the results of the offline optimization are shown.

Fig. 6. Dynamometer tests based on the real driving cycle B3.

actively supports the FCS in the high-power sections of the cycle, which avoids operating the FCS in its inefficient high-power range.

The effects of the two EMSs on the fuel efficiency are visually compared based on the equivalent fuel consumption, which takes into account the energy stored in the battery and is also shown in Fig. 6(b). Remarkably, the time courses of the equivalent fuel consumption of the two EMSs are almost identical in the initial 55 km of the driving cycle, indicating that potentially higher battery losses due to the increased battery use of the predictive SoC reference tracking are inconsiderable.

Table 3
Results of the dynamometer tests comparing the nonpredictive charge sustaining with the predictive SoC reference tracking.

(a) Real driving cycle B3.

	Charge sustaining	**SoC tracking**
Traction energy (kWh)	12.93	12.8
m_{eq} **(kg)**	**0.874**	**0.818**
Relative difference	**0%**	**−6.4%**
Mean FCS efficiency	50.1%	54.2%
Battery losses (kWh)	0.217	0.234

(b) WLTC.

	Charge sustaining	**SoC tracking**
Traction energy (kWh)	3.46	3.45
m_{eq} **(kg)**	**0.225**	**0.218**
Relative difference	**0%**	**−3.1%**
Mean FCS efficiency	51.8%	53.1%
Battery losses (kWh)	0.057	0.062

However, a significant gap between the equivalent consumption trajectories of the two strategies opens up during the high-power uphill sections on the freeway starting around 55 km, where the predictive SoC reference tracking successfully avoids the inefficient high-power FCS range.

The quantitative results are summarized in Table 3a and confirm these findings. The predictive SoC reference tracking reduces the equivalent fuel consumption by remarkable 6.4 % with respect to the nonpredictive charge sustaining. The dynamometer tests confirm that the reduction in the fuel consumption is based on an improvement in the mean FCS efficiency, which is significantly increased from 50.1 % for the charge sustaining strategy to 54.2 % for the predictive SoC reference tracking strategy. Compared to the nonpredictive strategy, the predictive SoC reference tracking produces higher ohmic battery losses because of the enhanced battery use, but this increase is of minor significance regarding the overall fuel efficiency, as already observed in the real driving tests. The outcomes confirm that long-term predictions derived from easily available static route information are highly effective for improving the fuel efficiency although their prediction quality is limited due to real-world disturbances. Also, the effectiveness of the simple and easily implementable real-time SoC reference tracking controller is confirmed.

5.2.2. Dynamometer tests based on the WLTC

The WLTC is a standard cycle for determining fuel consumption and emission levels. As such, the WLTC is a widely used test cycle in the literature, which is why it is interesting to evaluate the performance benefit of the predictive SoC reference tracking for the WLTC. However, one must keep in mind that the official test procedure does not consider the use of predictions, and thus, the WLTC tests are hypothetical tests here. Since speed limits are also not specified for the WLTC, the actual velocity reference for the dynamometer testbed is considered as theoretical velocity prediction (see Fig. 7(a)). However, vehicle standstills are considered unpredictable and therefore *not* represented in the prediction. Because the WLTC does not consider changes in altitude, this dynamometer test also investigates the potential of the predictive EMS for driving missions where the traction power profile is dominated by the velocity.

The close-to-ideal prediction offers the possibility to evaluate the accuracy of the long-term power demand prediction based on the vehicle dynamics. The predicted traction motor power estimates the measured traction motor power well (see Fig. 7(a)), confirming the suitability of the vehicle model. Only fast dynamics, i.e., the spikes in the measured traction motor power, are not represented due to the segmentation of the prediction for the offline optimization. However,

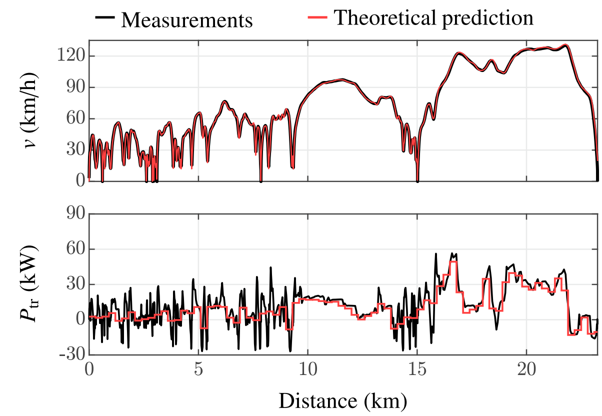

(a) Velocity and traction motor power of the WLTC. The velocity prediction coincides with the actual velocity, which is a theoretical test case.

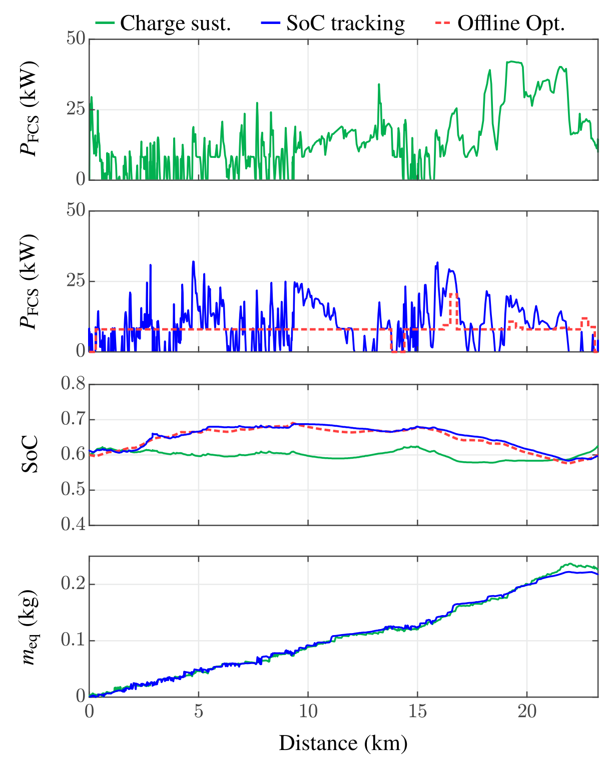

(b) Comparison of the nonpredictive charge sustaining strategy and the predictive SoC reference tracking. Additionally, the results of the offline optimization are shown.

Fig. 7. Dynamometer tests based on the WLTC.

this segmentation error does not limit the performance of the predictive concept because the real-time SoC tracking controller ensures enough freedom to deviate from the SoC reference optimized based on the prediction. Also, power demand spikes are assumed to be almost unpredictable in the real-world application.

The result of the offline optimization and the comparison of the two EMSs are shown in Fig. 7(b). Because of the relatively low mean power demand of the WLTC, the solution of the optimization indicates to operate the FCS mainly at the idle power limit. The corresponding SoC profile, which is used as reference for the predictive SoC reference tracking, basically plans to charge the battery in the initial low-power part of the cycle and discharge the battery in the final high-power part.

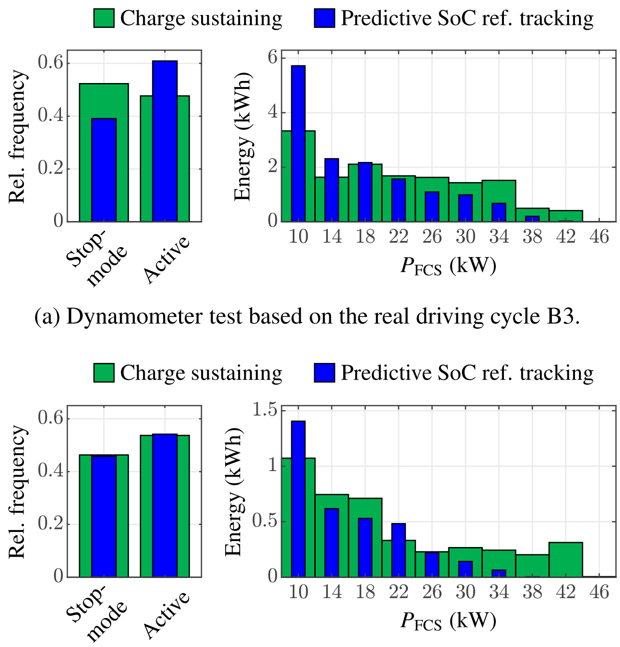

(a) Dynamometer test based on the real driving cycle B3.

(b) Dynamometer test based on the WLTC.

Fig. 8. Effects of the EMSs on the FCS operation: relative shares of the FCS operation modes (left plots) and the energy-weighted FCS power distribution (right plots).

The qualitative differences between the nonpredictive charge sustaining and the predictive SoC reference tracking are similar to the differences observed in the test based on the real driving cycle. Tracking the optimized SoC reference, the predictive SoC reference tracking considerably reduces high-power FCS operation compared to the charge sustaining strategy thanks to the active use of the battery, particularly in the final high-power section starting around 18 km. This is also where a significant difference in the equivalent fuel consumption graphs arises. Note that the equivalent fuel consumption decreases at the end of the test cycles because the battery is charged through regenerative breaking.

The quantitative results are summarized in Table 3b. The predictive SoC reference tracking strategy decreases the equivalent fuel consumption by 3.1 % with respect to the nonpredictive strategy. This result is notable and indicates that the predictive EMS can also bring significant improvements for driving missions without changes in altitude. The improvement again results from an increase in the mean FCS efficiency.

5.2.3. Analysis of the FCS power distribution

The effect of the predictive EMS on the FCS operation is analyzed in Fig. 8 for the two dynamometer tests. The histograms illustrate the energy-weighed FCS power distribution and confirm the aforementioned findings. Compared to the charge sustaining strategy, the predictive SoC reference tracking strategy shifts energy provided by high-power operation to low-power operation in both tests. Particularly the operation in the FCS power range just above the idle power limit, where the efficiency peaks, is significantly increased with the predictive EMS. For the dynamometer test based on the real driving cycle, the predictive SoC reference tracking also considerably reduces the time spent in the stopmode, which is beneficial because the mean FCS power in active operation is decreased in this way.

6. Conclusions

This work experimentally validated an easily implementable predictive EMS considering a long-term prediction derived from static route information to optimize a distance-based SoC reference trajectory before departure. Extensive experiments were conducted with a real fuel cell passenger vehicle on public roads and on a chassis dynamometer testbed. The real driving tests on public roads proofed the robustness of the predictive SoC reference tracking strategy in real driving situations affected by unpredicted disturbances such as varying traffic. Moreover, the real driving tests indicated a considerable reduction in the fuel consumption compared to a nonpredictive charge sustaining strategy with an average reduction of around 4.5 %. Reproducible dynamometer tests based on a selected real driving cycle, which included real-world traffic influences and vehicle standstills, confirmed these findings: Although these disturbances were not considered in the prediction, the predictive SoC reference tracking reduced the fuel consumption by remarkable 6.4 % compared to the nonpredictive charge sustaining. This result confirmed that simple, route-based long-term predictions are highly effective for improving the fuel efficiency in the real-world application, even though their accuracy is limited due to unpredictable random influences. Additionally, dynamometer tests based on the WLTC revealed a reduction in the fuel consumption by 3.1 % compared to the nonpredictive EMS. This result indicated that the predictive EMS can also improve the fuel efficiency for driving missions without changes in altitude. Finally, a detailed qualitative evaluation showed that the significant improvements arose by avoiding high FCS power ranges, which considerably increased the mean FCS efficiency.

CRediT authorship contribution statement

Sandro Kofler: Writing – original draft, Visualization, Validation, Software, Methodology, Investigation, Formal analysis, Data curation, Conceptualization. **Georg Rammer:** Software. **Alexander Schnabel:** Investigation, Data curation. **David Weingrill:** Investigation. **Peter Bardosch:** Supervision, Resources, Project administration, Funding acquisition. **Stefan Jakubek:** Writing – review & editing, Funding acquisition. **Christoph Hametner:** Writing – review & editing, Supervision, Project administration, Funding acquisition, Conceptualization.

Declaration of competing interest

The authors declare that they have no known competing financial interests or personal relationships that could have appeared to influence the work reported in this paper.

Acknowledgments

This work was supported with funds from the Climate and Energy Fund, Austria and implemented in line with the “Zero Emission Mobility” Program [grant numbers 878123, 885044]. The authors acknowledge the TU Wien Bibliothek for financial support through its Open Access Funding Program.

Data availability

The authors do not have permission to share data.

References

[1] X. Lin, Y. Xia, W. Huang, H. Li, Trip distance adaptive power prediction control strategy optimization for a plug-in fuel cell electric vehicle, Energy 224 (2021) 120232, http://dx.doi.org/10.1016/j.energy.2021.120232.

[2] Y. Liu, J. Li, Z. Chen, D. Qin, Y. Zhang, Research on a multi-objective hierarchical prediction energy management strategy for range extended fuel cell vehicles, J. Power Sources 429 (2019) 55–66, http://dx.doi.org/10.1016/j.jpowsour.2019.04.118.

[3] B. Geng, J.K. Mills, D. Sun, Two-stage energy management control of fuel cell plug-in hybrid electric vehicles considering fuel cell longevity, IEEE Trans. Veh. Technol. 61 (2) (2012) 498–508, http://dx.doi.org/10.1109/TVT.2011.2177483.

[4] Y. Zhou, A. Ravey, M.-C. Péra, A survey on driving prediction techniques for predictive energy management of plug-in hybrid electric vehicles, J. Power Sources 412 (2019) 480–495, http://dx.doi.org/10.1016/j.jpowsour.2018.11.085.
[5] S. Zendegan, A. Ferrara, S. Jakubek, C. Hametner, Predictive battery state of charge reference generation using basic route information for optimal energy management of heavy-duty fuel cell vehicles, IEEE Trans. Veh. Technol. 70 (12) (2021) 12517–12528, http://dx.doi.org/10.1109/TVT.2021.3121129.
[6] A. Ferrara, S. Jakubek, C. Hametner, Energy management of heavy-duty fuel cell vehicles in real-world driving scenarios: Robust design of strategies to maximize the hydrogen economy and system lifetime, Energy Convers. Manage. 232 (2021) 113795, http://dx.doi.org/10.1016/j.enconman.2020.113795.
[7] S. Gao, Y. Zong, F. Ju, Q. Wang, W. Huo, L. Wang, T. Wang, Scenario-oriented adaptive ECMS using speed prediction for fuel cell vehicles in real-world driving, Energy 304 (2024) 132028, http://dx.doi.org/10.1016/j.energy.2024.132028.
[8] H. Gao, Z. Wang, S. Yin, J. Lu, Z. Guo, W. Ma, Adaptive real-time optimal energy management strategy based on equivalent factors optimization for hybrid fuel cell system, Int. J. Hydrog. Energy 46 (5) (2021) 4329–4338, http://dx.doi.org/10.1016/j.ijhydene.2020.10.205.
[9] T. van Keulen, B. de Jager, A. Serrarens, M. Steinbuch, Optimal energy management in hybrid electric trucks using route information, Oil Gas Sci. Technol. – Rev. IFP 65 (1) (2010) 103–113, http://dx.doi.org/10.2516/ogst/2009026.
[10] M. Piras, V. De Bellis, E. Malfi, J.M. Desantes, R. Novella, M. Lopez-Juarez, Incorporating speed forecasting and SOC planning into predictive ecms for heavy-duty fuel cell vehicles, Int. J. Hydrog. Energy 55 (2024) 1405–1421, http://dx.doi.org/10.1016/j.ijhydene.2023.11.250.
[11] T. Zeng, C. Zhang, Y. Zhang, C. Deng, D. Hao, Z. Zhu, H. Ran, D. Cao, Optimization-oriented adaptive equivalent consumption minimization strategy based on short-term demand power prediction for fuel cell hybrid vehicle, Energy 227 (2021) 120305, http://dx.doi.org/10.1016/j.energy.2021.120305.
[12] D. Chen, Y. Kim, A.G. Stefanopoulou, Predictive equivalent consumption minimization strategy with segmented traffic information, IEEE Trans. Veh. Technol. 69 (12) (2020) 14377–14390, http://dx.doi.org/10.1109/TVT.2020.3034552.
[13] F. Zhang, K. Xu, C. Zhou, S. Han, H. Pang, Y. Cui, Predictive equivalent consumption minimization strategy for hybrid electric vehicles, in: 2019 IEEE Vehicle Power and Propulsion Conference, VPPC, 2019, pp. 1–5, http://dx.doi.org/10.1109/VPPC46532.2019.8952549.
[14] X. Li, Y. Wang, D. Yang, Z. Chen, Adaptive energy management strategy for fuel cell/battery hybrid vehicles using pontryagin's minimal principle, J. Power Sources 440 (2019) 227105, http://dx.doi.org/10.1016/j.jpowsour.2019.227105.
[15] X. Lin, X. Xu, H. Lin, Predictive-ECMS based degradation protective control strategy for a fuel cell hybrid electric vehicle considering uphill condition, eTransportation 12 (2022) 100168, http://dx.doi.org/10.1016/j.etran.2022.100168.
[16] D.F. Pereira, F.d.C. Lopes, E.H. Watanabe, Nonlinear model predictive control for the energy management of fuel cell hybrid electric vehicles in real time, IEEE Trans. Ind. Electron. 68 (4) (2021) 3213–3223, http://dx.doi.org/10.1109/TIE.2020.2979528.
[17] X. Zhang, L. Guo, N. Guo, Y. Zou, G. Du, Bi-level energy management of plug-in hybrid electric vehicles for fuel economy and battery lifetime with intelligent state-of-charge reference, J. Power Sources 481 (2021) 228798, http://dx.doi.org/10.1016/j.jpowsour.2020.228798.
[18] Y. Zhou, H. Li, A. Ravey, M.-C. Péra, An integrated predictive energy management for light-duty range-extended plug-in fuel cell electric vehicle, J. Power Sources 451 (2020) 227780, http://dx.doi.org/10.1016/j.jpowsour.2020.227780.
[19] G. Li, J. Zhang, H. He, Battery SOC constraint comparison for predictive energy management of plug-in hybrid electric bus, Appl. Energy 194 (2017) 578–587, http://dx.doi.org/10.1016/j.apenergy.2016.09.071.
[20] S. Kofler, S. Jakubek, C. Hametner, Cost-to-go-based predictive equivalent consumption minimization strategy for fuel cell vehicles considering route information, in: 2024 IEEE Intelligent Vehicles Symposium, IV, 2024, pp. 2910–2916, http://dx.doi.org/10.1109/IV55156.2024.10588715.
[21] S. Kofler, S. Jakubek, C. Hametner, Predictive energy management strategy with optimal stack start/stop control for fuel cell vehicles, Appl. Energy 377 (2025) 124513, http://dx.doi.org/10.1016/j.apenergy.2024.124513.
[22] C. Zhang, A. Vahidi, Route preview in energy management of plug-in hybrid vehicles, IEEE Trans. Control Syst. Technol. 20 (2) (2012) 546–553, http://dx.doi.org/10.1109/TCST.2011.2115242.
[23] S. Kofler, Z.P. Du, S. Jakubek, C. Hametner, Predictive energy management strategy for fuel cell vehicles combining long-term and short-term forecasts, IEEE Trans. Veh. Technol. (2024) 1–11, http://dx.doi.org/10.1109/TVT.2024.3424422.
[24] W. Zou, J. Li, Q. Yang, X. Wan, Y. He, H. Lan, A real-time energy management approach with fuel cell and battery competition-synergy control for the fuel cell vehicle, Appl. Energy 334 (2023) 120667, http://dx.doi.org/10.1016/j.apenergy.2023.120667.
[25] S. Quan, Y.-X. Wang, X. Xiao, H. He, F. Sun, Real-time energy management for fuel cell electric vehicle using speed prediction-based model predictive control considering performance degradation, Appl. Energy 304 (2021) 117845, http://dx.doi.org/10.1016/j.apenergy.2021.117845.
[26] Z. Sun, Y. Wang, Z. Chen, Coordination control strategy for PEM fuel cell system considering vehicle velocity prediction information, eTransportation 18 (2023) 100287, http://dx.doi.org/10.1016/j.etran.2023.100287.
[27] M. Kandidayeni, A.O. Macias Fernandez, A. Khalatbarisoltani, L. Boulon, S. Kelouwani, H. Chaoui, An online energy management strategy for a fuel cell/battery vehicle considering the driving pattern and performance drift impacts, IEEE Trans. Veh. Technol. 68 (12) (2019) 11427–11438, http://dx.doi.org/10.1109/TVT.2019.2936713.
[28] C. Jia, W. Qiao, J. Cui, L. Qu, Adaptive model-predictive-control-based real-time energy management of fuel cell hybrid electric vehicles, IEEE Trans. Power Electron. 38 (2) (2023) 2681–2694, http://dx.doi.org/10.1109/TPEL.2022.3214782.
[29] H. Chen, J. Chen, H. Lu, C. Yan, Z. Liu, A modified MPC-based optimal strategy of power management for fuel cell hybrid vehicles, IEEE/ASME Trans. Mechatronics 25 (4) (2020) 2009–2018, http://dx.doi.org/10.1109/TMECH.2020.2993811.
[30] D. Zhou, A. Al-Durra, F. Gao, A. Ravey, I. Matraji, M. Godoy Simões, Online energy management strategy of fuel cell hybrid electric vehicles based on data fusion approach, J. Power Sources 366 (2017) 278–291, http://dx.doi.org/10.1016/j.jpowsour.2017.08.107.
[31] C. Varlese, A. Ferrara, C. Hametner, P. Hofmann, Experimental validation of a predictive energy management strategy for agricultural fuel cell electric tractors, Int. J. Hydrog. Energy 77 (2024) 1–14, http://dx.doi.org/10.1016/j.ijhydene.2024.06.097.
[32] K. Deng, H. Peng, S. Dirkes, J. Gottschalk, C. Ünlübayir, A. Thul, L. Löwenstein, S. Pischinger, K. Hameyer, An adaptive PMP-based model predictive energy management strategy for fuel cell hybrid railway vehicles, eTransportation 7 (2021) 100094, http://dx.doi.org/10.1016/j.etran.2020.100094.
[33] H. Peng, Z. Chen, K. Deng, S. Dirkes, C. Ünlübayir, A. Thul, L. Löwenstein, D.U. Sauer, S. Pischinger, K. Hameyer, A comparison of various universally applicable power distribution strategies for fuel cell hybrid trains utilizing component modeling at different levels of detail: From simulation to test bench measurement, eTransportation 9 (2021) 100120, http://dx.doi.org/10.1016/j.etran.2021.100120.
[34] A. Ravey, B. Blunier, A. Miraoui, Control strategies for fuel-cell-based hybrid electric vehicles: From offline to online and experimental results, IEEE Trans. Veh. Technol. 61 (6) (2012) 2452–2457, http://dx.doi.org/10.1109/TVT.2012.2198680.
[35] Y. Zhang, R. Ma, D. Zhao, Y. Huangfu, W. Liu, A novel energy management strategy based on dual reward function Q-learning for fuel cell hybrid electric vehicle, IEEE Trans. Ind. Electron. 69 (2) (2022) 1537–1547, http://dx.doi.org/10.1109/TIE.2021.3062273.
[36] J. Chen, C. Xu, C. Wu, W. Xu, Adaptive fuzzy logic control of fuel-cell-battery hybrid systems for electric vehicles, IEEE Trans. Ind. Inform. 14 (1) (2018) 292–300, http://dx.doi.org/10.1109/TII.2016.2618886.
[37] G. Şefkat, M.A. Özel, Experimental and numerical study of energy and thermal management system for a hydrogen fuel cell-battery hybrid electric vehicle, Energy 238 (2022) 121794, http://dx.doi.org/10.1016/j.energy.2021.121794.
[38] M. Sellali, A. Ravey, A. Betka, A. Kouzou, M. Benbouzid, A. Djerdir, R. Kennel, M. Abdelrahem, Multi-objective optimization-based health-conscious predictive energy management strategy for fuel cell hybrid electric vehicles, Energies 15 (4) (2022) http://dx.doi.org/10.3390/en15041318.
[39] D. Gao, Z. Jin, Q. Lu, Energy management strategy based on fuzzy logic for a fuel cell hybrid bus, J. Power Sources 185 (1) (2008) 311–317, http://dx.doi.org/10.1016/j.jpowsour.2008.06.083.
[40] X. Li, L. Xu, J. Hua, X. Lin, J. Li, M. Ouyang, Power management strategy for vehicular-applied hybrid fuel cell/battery power system, J. Power Sources 191 (2) (2009) 542–549, http://dx.doi.org/10.1016/j.jpowsour.2009.01.092.
[41] C. Geng, S. Mei, L. Liu, W. Ma, Q. Xue, Simulation and experimental research on energy management control strategy for fuel cell heavy-duty truck, Int. J. Hydrog. Energy 69 (2024) 1305–1318, http://dx.doi.org/10.1016/j.ijhydene.2024.05.081.
[42] Z. Hu, J. Li, L. Xu, Z. Song, C. Fang, M. Ouyang, G. Dou, G. Kou, Multi-objective energy management optimization and parameter sizing for proton exchange membrane hybrid fuel cell vehicles, Energy Convers. Manage. 129 (2016) 108–121, http://dx.doi.org/10.1016/j.enconman.2016.09.082.
[43] L. Xu, J. Li, M. Ouyang, Energy flow modeling and real-time control design basing on mean values for maximizing driving mileage of a fuel cell bus, Int. J. Hydrog. Energy 40 (43) (2015) 15052–15066, http://dx.doi.org/10.1016/j.ijhydene.2015.08.104.
[44] L. Xu, J. Li, J. Hua, X. Li, M. Ouyang, Adaptive supervisory control strategy of a fuel cell/battery-powered city bus, J. Power Sources 194 (1) (2009) 360–368, http://dx.doi.org/10.1016/j.jpowsour.2009.04.074, XIth Polish Conference on Fast Ionic Conductors 2008.
[45] P. Bubna, D. Brunner, S.G. Advani, A.K. Prasad, Prediction-based optimal power management in a fuel cell/battery plug-in hybrid vehicle, J. Power Sources 195 (19) (2010) 6699–6708, http://dx.doi.org/10.1016/j.jpowsour.2010.04.008.
[46] L. Guzzella, A. Sciarretta, Vehicle Propulsion Systems: Introduction to Modeling and Optimization, Springer, Berlin, Heidelberg, 2013, http://dx.doi.org/10.1007/978-3-642-35913-2.